Iranian Society of Acoustics and Vibration
The 12th International Conference on Acoustics and Vibration ISAV2022
14-15 Dec 2022 Tehran - Iran
Amirkabir University of Technology

Vibration dynamics analysis of a washing machine cabinet using efficient topography

Ali Tofangsaz[a], Ramin Jahadi[a,b*]

[a] *Sound and Vibration Research Center, Department of Research and Development, Entekhab Industrial Group, Morcheh Khort Industrial Zone, P.O. Box 83315-313, Isfahan, Iran.*

[b] *PhD, Department of Mechanical Engineering, Faculty of Engineering, University of Isfahan, 81746-73441, Isfahan,Iran*

** Corresponding author e-mail: jahadi.r@entekhabgroup.com*

Abstract

Washing machines are complex dynamic systems that can undergo severe vibratory forces during their Spin cycles due to the non-uniform distribution of load in their drums. Being mass-produced consumer products, the application of most vibration attenuation methods, especially active ones, is not financially feasible. Optimization of side patterns is a cost-effective candidate for passive vibration attenuation in washing machines. In this study, different approaches to FEM analysis and modelling were studied and FEM analyses were performed on two different side patterns. This was done with the goal of developing efficient and cost-effective tools for reaching an optimum topography design during the product development phase. To verify these analyses and their accuracy, the results obtained from FEM analyses were compared with the results of modal tests performed on prototype products with the two side patterns. In addition, to estimate the effectiveness of side pattern design on vibration attenuation, the body vibration of these two prototype products was measured and compared. The results show that FEM analyses can be used to reach a relatively accurate estimate of side panel natural frequencies with a maximum error margin of 5.2%. It is also shown that side pattern design directly affect the washing machine's cabin stiffness and natural frequencies, and it was observed that proper topography can increase side panel natural frequencies up to 58%. This increase in natural frequencies, in turn, resulted in a 27% reduction in peak body displacement of the washing machine's cabin vibration during the Spin cycle.

Keywords: Vibration Attenuation; Modal Analysis; FEM; Washing machine.

1. Introduction

Despite their apparent simplicity, washing machines are complex dynamic machines that harbour a myriad of design and analysis difficulties. These difficulties include but are not limited to load uncertainties, non-linear components, and low natural frequencies that lie below or inside the machine's working range. A washing machine can be divided into two primary assemblies. The first to which is a cabin assembly containing the metal cabin, door assembly, regulating feet, etc. Most of

these parts are static components, and except for the drain and circulation pumps, the other components of this group are not sources of noise and vibration themselves. The main source of noise and vibration in a washing machine is the second assembly. This includes the tub, drum, motor, balancing weights, etc. This assembly is suspended from the cabin top with the aid of several extension springs and is connected to the bottom of the cabin via friction dampers. Fig. 1 shows the relation between the two assemblies. Until recent years, almost all efforts in noise and vibration reduction of washing machines were focused on optimizing tub assembly through multibody models, as represented by Nygårds et al. [1]. However, most solutions offered by these studies are not financially feasible. The use of patterned side panels in washing machine cabin design can be a cost-effective method for the reduction and control of washing machine body vibrations and emitted noise.

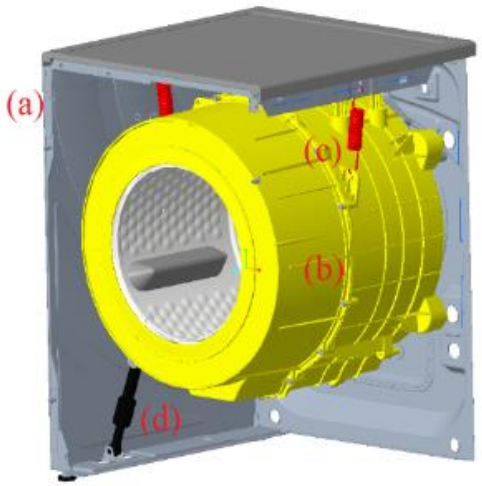

Figure 1. The relation between and relative positions of (a) Cabin Assembly, (b) Tub Assembly, (c) Tub springs, and (d) dampers in a typical washing machine.

It is known that the stiffness and natural frequency of a sheet metal plate can be increased by embossing and creating patterns during the stamping process. Namoco [2] proved that embossing and restoration techniques could increase the stiffness and strength of sheet metals. Nama et al. [3] showed that the natural frequency of a thin rectangular plate could be increased up to 23% using an array of dimples on the surface. Kim et al. [4] used optimization techniques to reach an optimal topography for depressions in enclosure panels of a compressor to reduce emitted airborne noise. Similar techniques have been proposed in washing machines to increase the stiffness and natural frequencies of cabin assembly. Yong et al. [5] studied the effects of two side patterns on cabin's natural frequencies using a verified FEM model. It was estimated that the new proposed design would result in a 19% reduction in vibration amplitude. Kim et al. [6] used an initially verified FEM model and optimization techniques to reach an optimized topography for washing machine side patterns.

Although the works mentioned above have used some experiments on initial designs of side panel topographies to verify their FEM models, they have not verified the effectiveness of their proposed improvements through experiments. The following work aims to (a) determine the effects of side patterns on the natural frequencies and mode shapes of the washing machine cabin and (b) subsequent effects of side pattern design on body vibration during the Spin cycle through both FEM analyses and experiments. In the first part of this study, the natural frequencies and mode shapes of side panels with two proposed patterns are estimated using the FEM method with the help of ABAQUS/CAE commercial finite element software. These estimates are later verified by performing modal tests on washing machines with prototype cabin assemblies. Finally, the effects of the side patterns on body vibrations and their effectiveness in vibration attenuation are measured through body vibration measurement tests.

2. General discussion

2.1 Theoretical Basis

Each of the washing machine side panels can be considered as a rectangular plate with clamped-simple boundary conditions. In this regard, as is demonstrated in Fasihi et al. [7], governing equations of the patterned plate can be obtained using thin plate theory and the principle of superposition. Fig. 2 depicts one possible procedure used to acquire the governing equations.

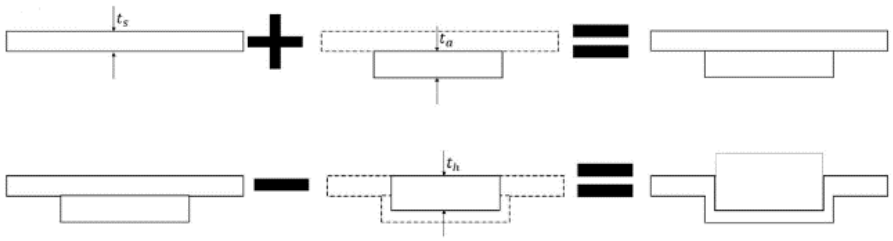

Figure 2. Schematic procedure for the use of superposition principle in obtaining governing equations [7].

The kinetic and potential energy of the side panels can be calculated using Eq. (1), where T and U represent kinetic and potential energies respectively, ρ is the panel's density, ν is the Poisson's ratio of the panel's material, w is the element's lateral displacement, a, b, and t are dimensions of the side panel, t being its thickness. Using the superposition principle, the mass and stiffness matrices can be calculated utilizing Eq. (2) for each of the respective elements. In these equations, Φ_i and Φ_j are orthogonal admissible functions, ζ and ξ are non-dimensional spatial coordinates, D is flexural rigidity, and M_{sij} and K_{sij} are elements mass and stiffness matrices respectively. The resulting mass and stiffness matrices are used in Eq. (3) to obtain the overall mass and stiffness matrices.

$$T_s = \frac{1}{2}\rho t_s \int_0^{a_s}\int_0^{b_s} \dot{w}^2 dxdy\,,$$
$$U_s = \frac{1}{2}D_s \int_0^{a_s}\int_0^{b_s}\left[\left(\frac{\partial^2 w}{\partial x^2}\right)^2 + \left(\frac{\partial^2 w}{\partial y^2}\right)^2 + 2\nu\left(\frac{\partial^2 w}{\partial x^2}\frac{\partial^2 w}{\partial y^2}\right) + 2(1-\nu)\left(\frac{\partial^2 w}{\partial x \partial y}\right)\right] dxdy \quad (1)$$

$$M_{sij} = \rho t_s a_s b_s \int_0^1\int_0^1 \Phi_i \Phi_j d\zeta d\xi\,,$$
$$K_{sij} = \frac{D_s b_s}{a_s^3}\int_0^1\int_0^1\left[\frac{\partial^2\Phi_i}{\partial\zeta^2}\frac{\partial^2\Phi_j}{\partial\zeta^2} + \alpha^4\frac{\partial^2\Phi_i}{\partial\xi^2}\frac{\partial^2\Phi_j}{\partial\xi^2} + \nu\alpha^2\left(\frac{\partial^2\Phi_i}{\partial\zeta^2}\frac{\partial^2\Phi_j}{\partial\xi^2} + \frac{\partial^2\Phi_i}{\partial\xi^2}\frac{\partial^2\Phi_j}{\partial\zeta^2}\right)\right. \quad (2)$$
$$\left. + 2(1-\nu)\alpha^2\frac{\partial^2\Phi_i}{\partial\zeta\partial\xi}\frac{\partial^2\Phi_j}{\partial\zeta\partial\xi}\right] d\zeta d\xi \quad , i,j = 1,2,3,\dots,m \quad , \quad \alpha = \frac{a_s}{b_s}.$$

$$\mathbf{M} = \mathbf{M}_s + \sum_{f=1}^{n_p}\left(\mathbf{M}_{af} - \mathbf{M}_{hf}\right) \quad , \quad \mathbf{K} = \mathbf{K}_s + \sum_{f=1}^{n_p}\left(\mathbf{K}_{af} - \mathbf{K}_{hf}\right) \quad (3)$$

Applying the clamped-simple boundary conditions will result in the following equation, which then will be inserted into elements of Eq. (2) to form the integral required for the calculation of mass and stiffness elements.

$$\varphi_i(\zeta) = cosh(\lambda_i\zeta) - cos(\lambda_i\zeta) - \sigma_i\left(sinh(\lambda_i\zeta) - sin(\lambda_i\zeta)\right)$$
$$\lambda_i = \lambda_i = (4i+1)\frac{\pi}{4}\ for\ i > 5 \quad , \quad \sigma_i = \frac{cosh(\lambda_i) - cos(\lambda_i)}{sinh(\lambda_i) - sin(\lambda_i)} \quad (4)$$

As is presented in [7], this approach has yielded promising results, and the resulting equations are extremely useful in evaluating the effects of different design parameters on the overall performance of the side panels and in gaining a ballpark estimate of properties such as mode shapes and natural frequencies. However, this is a cumbersome method, and its use becomes ever increasingly difficult as the side panel topographies becomes ever more complicated. Thus, to analyse side panels with complex topographies, other methods must be utilized.

2.2 Finite Element Modelling

In this work, FEM analyses have been performed using two different approaches. The first approach is an agile method in which only an isolated side panel is modelled, while the second approach focuses on a more comprehensive model of the whole cabin assembly. The results of the analyses are compared and verified via experiments in section 2.3.

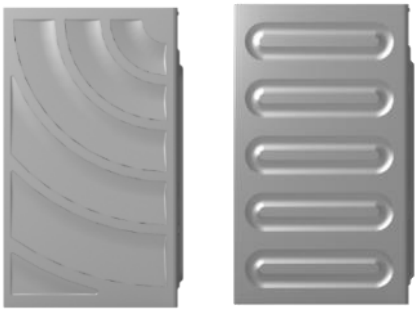

Pattern (a) Pattern (b)

Figure 2. Renderings of the two side panel topographies under study, pattern (a), also referred to as "Wi-Fi pattern" (left), and pattern (b), also referred to as "beads pattern" (right).

For FEM analyses, models of both the whole cabin assembly and the isolated side panels were created. Fig. 3 shows the 3D renderings of the two models. To mesh the models, standard quadratic tetrahedral solid elements (C3D10) were used and mesh dependence studies were performed. Fig. 4 illustrates the results of the mesh dependence studies. For steel parts such as side panels, a Young's modulus of 200 GPa, a density of 7800 Kg/m^3, and a Poisson's ratio of 0.3, and for plastic parts, the mechanical properties of Polypropylene were used (E=1.4 GPa, ρ=900 Kg/m^3, ν=0.4).

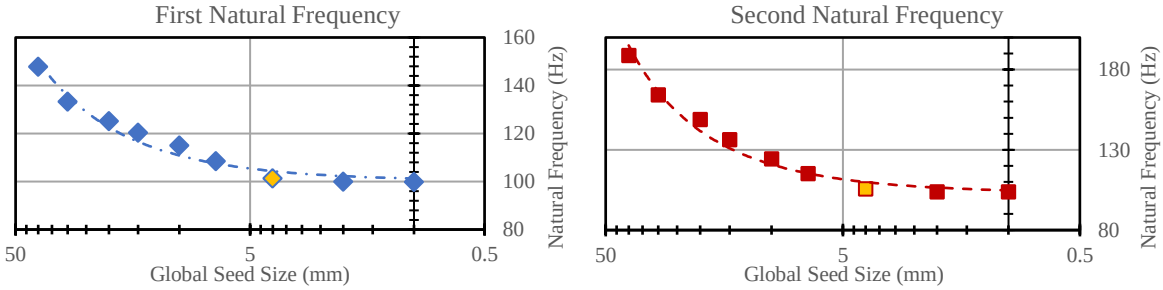

Figure 4. The results of mesh dependence analysis on first (left) and second (right) natural frequencies.

2.2.1 FEM Analysis of the Isolated Side Panels

In the first approach, only one of the side panels is modelled in isolation. To model the boundary conditions, on the left and right sides, clamped boundary conditions, and on the top and bottom sides, hinged boundary conditions were used. Table 1 shows the mode shapes and natural frequencies of the isolated side panels with two different topographies. As the results show, the beads pattern (b) exhibited higher natural frequencies, and thus it is expected that cabins with this pattern will have better overall vibrational performance.

Table 1. The results of FEM analysis of the isolated side panels.

Pattern a (Wi-Fi pattern)			Pattern b (beads pattern)		
Mode Type	Natural Frequency (Hz)	Mode Shape	Mode Type	Natural Frequency (Hz)	Mode Shape
1,1	72.86	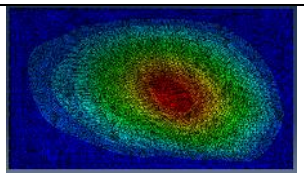	1,1	101.28	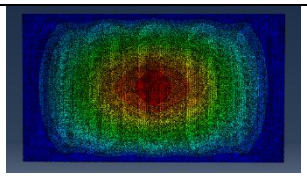

2,1	89.40	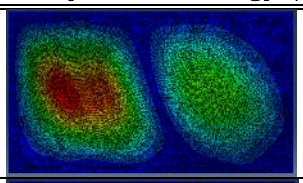	2,1	105.59	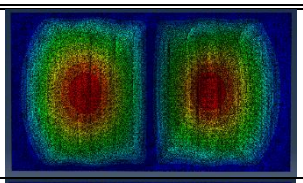
3,1	110.47	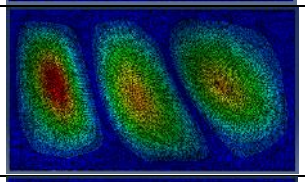	3,1	113.82	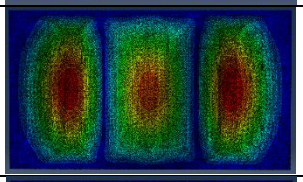
4,1	143.43	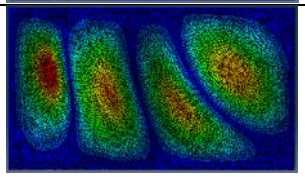	4,1	126.67	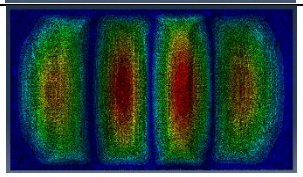

2.2.2 FEM Analysis of the Whole Cabin Assembly

Despite all efforts to accurately model the side panel boundary conditions, it is nearly impossible to do so. Since, in reality, the side panel boundary conditions are neither free nor completely fixed, but something in between, and determining each boundary's stiffness is a rather complicated deal. Thus, it is much more feasible to model the entire cabin assembly. Table 2 shows the mode shapes and natural frequencies of the two patterns resulting from the analysis of the whole cabin assembly. As it is evident from the comparison of Tables 1 and 2, the two analyses resulted in both a different sequence of mode shapes and different natural frequencies for similar mode shapes.

Table 2. The results of FEM analysis of the whole cabin assembly.

Pattern a (Wi-Fi pattern)			Pattern b (beads pattern)		
Mode Type	Natural Frequency (Hz)	Mode Shape	Mode Type	Natural Frequency (Hz)	Mode Shape
1,1	43.17	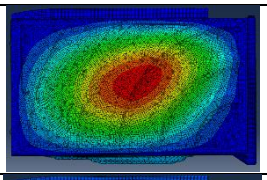	1,1	50.06	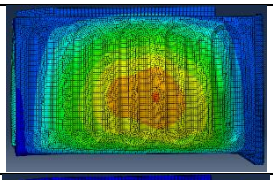
2,1	58.06	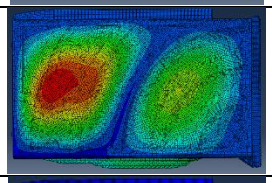	2,1	64.76	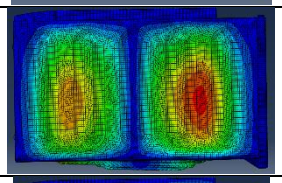
3,1	79.24	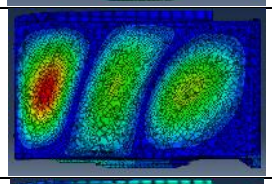	3,1	82.49	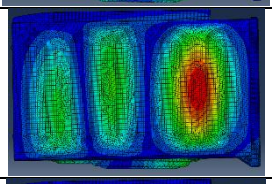
2,2	104.17	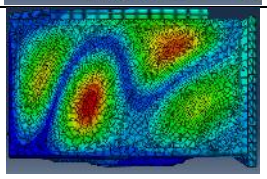	4,1	98.04	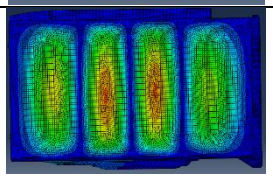

2.3 Experiments

To verify the frequency analyses using the FEM method, two experimental studies were performed on the complete washing machines with prototype cabins, in which each of these cabins used one of the previously analysed side panel topographies. In the first study, modal tests were

performed on the side panels, and the resulting natural frequencies and mode shapes were compared with the FEM analyses. In the second study, to evaluate the effectiveness of side patterns on vibration attenuation, body vibrations of the washing machines were measured under similar working conditions. Table 3 is a list of the equipment used in the experimental studies.

Table 3. List of Equipment used in the experimental studies.

Name	Manufacturer	Model	Calibration Due Date
Uniaxial Accelerometer	PCB Piezotronics	352A56	2022/08
Modal Impact Hammer	PCB Piezotronics	086C03	2022/10
Handheld Accelerometer Calibrator	PCB Piezotronics	394C06	2023/04
Data Acquisition System	M+P	VP4	2023/10
Data Acquisition System	M+P	VP8	2023/10
Temperature and Humidity Data Logger	TESTO	175H1	2023/06

2.3.1 Modal Test

The following modal tests were conducted in compliance with ISO 7626-5: 2019 [8]. First, a mesh grid was created on the side panels of each prototype, and then the tests were performed using the sensor roaming technique. Accordingly, in each step, the sensors were moved sequentially through the nodes while the impact point remained fixed at a single node. At each step, the sensors were attached to the side panels in accordance with ISO 5348:2021 [9]. The environmental conditions were monitored and controlled during the test in compliance with requirements mentioned in part 5.7 of ISO 2954 [10] and part 4.6.2 of ISA-TR52.00.01 (2006) [11]. Fig. 5 shows both the mesh grid and the test set-up used for the modal analysis of the prototype cabins with the two different topographies.

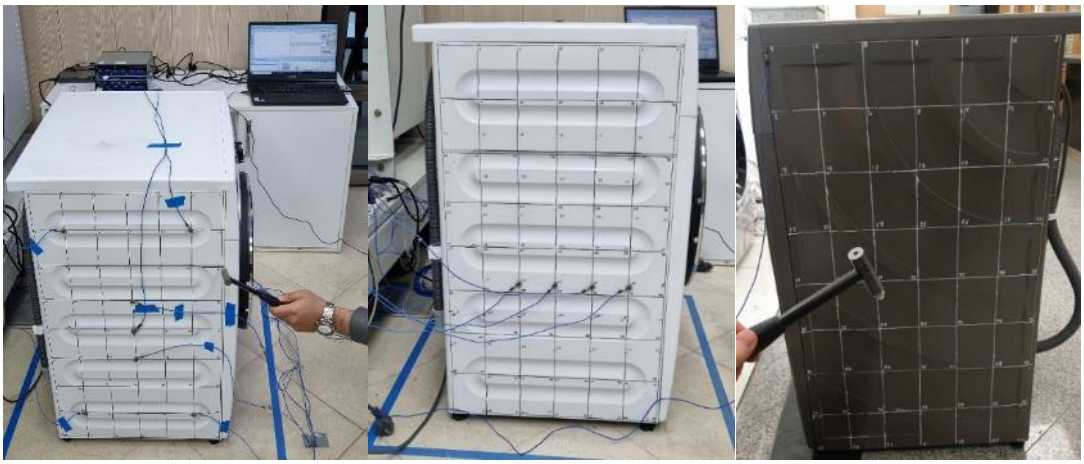

Figure 5. Test set-up and mesh grid applied on the side panels of prototype cabins.

The comparative results of the modal analyses performed on the two side patterns are reported in Table 4. Based on these results, the following conclusions can be made:

1) The prototype with beads pattern (b) demonstrated higher natural frequencies, and compared to Wi-Fi pattern (a), an increase of 89%, 56%, and 34% was observed in its first three natural frequencies, respectively. These results indicate that the beads pattern was able to increase side panel stiffness to a greater degree. Therefore, it is expected that cabins with this side panel will have better vibrational performance.

2) The sequence of mode shapes and the natural frequencies of each mode shape is closer to the results obtained from the FEM analysis of the whole cabin assembly. Compared to the modal test results, the first three natural frequencies obtained from FEM analysis of the isolated side panels had an error of 139%, 87%, and 51%, respectively. All the while, the average error for the first three natural frequencies obtained from the analysis of the whole cabin assembly for the beads pattern were 0.02%, -1.01%, and -5.18%. The errors for whole cabin assembly analysis of the Wi-Fi pattern, although higher are still considerably lower than the error margins for isolated side panels' analyses.

Therefore, to reach a more accurate estimate of the natural frequency and mode shapes of the side panels, the whole cabin assembly must be modelled and analysed.

Table 4. The results of modal analysis tests performed on prototype washing machines.

	Pattern a (Wi-Fi pattern)		Pattern b (beads pattern)	
Mode Type	Natural Frequency (Hz)	Mode Shape	Natural Frequency (Hz)	Mode Shape
1,1	26.48	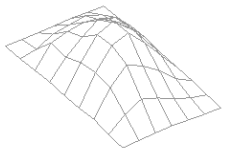	50.05	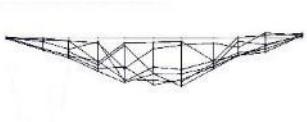
2,1	41.91	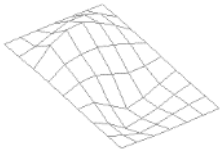	65.42	
3,1	64.80	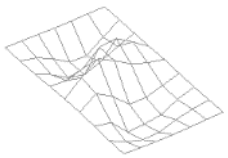	87.00	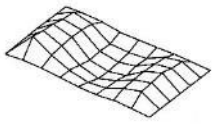
2,2	108.22	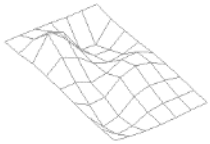	163.28	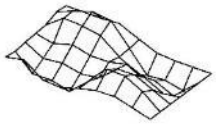

2.3.2 Body Vibration Measurement

To measure the effects of side patterns on washing machine vibrations during the Spin cycle, two washing machines with prototype cabins were tested with a test method based on ISO 20816-1:2016 [12] and ISO 2954:2012 [10]. To recreate a forced vibration situation similar to what a washing machine undergoes during its Spin cycle with a load that has non-uniform distribution, magnets were placed inside the drum. Six uniaxial accelerometers were installed on the washing machine side panels.

The body vibration (peak displacement) was measured in the Spin cycle when the washing machine reached its maximum rotation speed. Care was taken to ensure that the washing machine had reached a stable condition prior to each reading. Table 5 summarizes the results obtained from the body vibration measurement performed on washing machines. For an easy comparison of the performance of the two side patterns, the RMS of the values was also calculated.

Table 5. Summary of body vibration results.

Side pattern design	Unbalance Load (g)	Peak Displacement (mm)						
		Left			Right			RMS
		Top	Middle	Bottom	Top	Middle	Bottom	
Pattern a	330	0.19	0.07	0.05	0.20	0.19	0.08	0.15
Pattern b	330	0.13	0.08	0.09	0.15	0.08	0.03	0.10
Pattern a	385	0.19	0.06	0.04	0.18	0.18	0.09	0.14
Pattern b	385	0.15	0.08	0.08	0.16	0.09	0.04	0.11

As is evident from the data presented in Table 4, the beads pattern (b), with a higher natural frequency and stiffness, demonstrated on average, a 27% reduction in peak body vibration. It is

expected that the decrease in body vibration, in addition to directly enhancing the customer experience, will in turn, reduce the washing machine's airborne noise levels. This is due to the presence of a strong vibroacoustic effect in washing machines.

3. Conclusion

It can be concluded that the optimization of side patterns is an efficient and cost-effective method for vibration attenuation. In addition, it was observed that FEM analysis could be a quick and relatively accurate method for evaluating and predicting the performance of different side patterns during the design phase, reducing the need for prototype manufacture and testing. However, it was noted that to reach accurate results, modelling of the isolated side panels is not sufficient, and the whole cabin assembly must be modelled. It was shown that FEM analyses of the whole cabin assembly, in comparison to the results of experimental modal tests could lead to quite accurate results, with a maximum error margin of 5.2%. Accordingly, the numerical results are in good agreement with the experimental values. The experiments showed that prototype cabins with bead pattern (b) topography had higher natural frequencies compared to cabins with Wi-Fi pattern (a), and on average, a 58% increase in natural frequency was observed. Similarly, a 27% reduction in peak body vibration was observed in cabins with type (b) side pattern. Thus, it has been established that an apparent direct relationship is present between the natural frequencies of side panels and the washing machine's body peak displacement during the Spin cycle. Further studies are needed to determine the possible effects of side patterns on the airborne noise levels of the washing machine.

REFERENCES

1. T. Nygårds, V. Berbyuk, "Multibody modeling and vibration dynamics analysis of washing machines", *Multibody System Dynamics* **27.2**, 197-238 (2012).
2. C. S. Namoco, "Improving the rigidity of sheet metal by embossing and restoration technique", *Mindanao Journal of Science and Technology* **8** (2010).
3. S. A. Nama, S. M. Khazaal, "Investigating the Effect of Embossing and Restoration Process on The Natural Frequency of Rectangular Plate", *Journal of Mechanical Engineering Research and Developments* **44.1**, 75-82 (2020).
4. H. G. Kim, C. Nerse, and S. Wang, "Topography optimization of an enclosure panel for low-frequency noise and vibration reduction using the equivalent radiated power approach", *Materials & Design* **183**, 108-125 (2019).
5. S. J. Yong, K. H. Kim, and Y. G. Kim, "Cabinet design for vibration reduction of a drum type washing machine", *Journal of the Korean Society for Precision Engineering* **33.9**, 731-737 (2016).
6. H. G. Kim, et al., "Efficient topography optimization of a washing machine cabinet to reduce radiated noise during the dehydration process", *Journal of Mechanical Science and Technology* **35.3**, 973-978 (2021).
7. M.H. Fasihi Harandi, A. Loghmani, "Theoretical and Experimental Investigation of Free Vibrations of Rectangular Plates with Vertical Patterns", *Iranian Journal of Science and Technology, Transactions of Mechanical Engineering*, 1-15 (2022).
8. International Organization for Standardization. (2019). "Mechanical vibration and shock — Experimental determination of mechanical mobility — Part 5: Measurements using impact excitation with an exciter which is not attached to the structure", (ISO Standard No. 7626-5:2019). https://www.iso.org/standard/68735.html
9. International Organization for Standardization. (2021). "Mechanical vibration and shock — Mechanical mounting of accelerometers", (ISO Standard No. 5348:2021). https://www.iso.org/standard/78160.html
10. International Organization for Standardization. (2012). "Mechanical vibration of rotating and reciprocating machinery — Requirements for instruments for measuring vibration severity", (ISO Standard No. 2954:2012). https://www.iso.org/standard/21835.html
11. International Society of Automation. (2006). "Recommended Environments for Standards Laboratories", (ISA Document No. TR52.00.01-2006). https://www.isa.org/products/isa-tr52-00-01-2006-recommended-environments-for-s
12. International Organization for Standardization. (2016). "Mechanical vibration — Measurement and evaluation of machine vibration — Part 1: General guidelines", (ISO Standard No. 20816-1:2016). https://www.iso.org/standard/63180.html